B. London, J. C. Shyne,* and D. V. Nelson†*

Small Fatigue Crack Behaviour Monitored Using Surface Acoustic Waves in Quenched and Tempered 4140 Steel

REFERENCE London, B., Shyne, J. C., and Nelson, D. V., **Small Fatigue Crack Behaviour Monitoried Using Surface Acoustic Waves in Quenched and Tempered 4140 Steel,** *The Behaviour of Short Fatigue Cracks*, EGF Pub. 1 (Edited by K. J. Miller and E. R. de los Rios) 1986, Mechanical Engineering Publications, London, pp. 537–552.

ABSTRACT A surface acoustic wave ultrasonic technique employed to monitor the growth of small surface fatigue cracks is briefly described. The technique allows accurate measurement of crack depth and rapid determination of the crack closure stress. The closure stress determined acoustically is shown to correlate well with that measured by monitoring the crack tip opening displacement versus applied stress in an SEM. Semi-circular surface cracks from 70 to 250 μm in depth and long through cracks in compact tension samples were studied in high purity 4140 steel. Tempering temperature was used to vary the yield strength and microstructure of the specimens. Samples were tempered at 200,400,550, or 700°C producing a range of yield strengths from 875 to 1600 MPa, respectively. Small surface cracks were initiated from a 25 to 40 μm deep surface pit in specially designed cantilevered bending fatigue specimens. The effects of tempering temperature on both long and small fatigue crack growth are presented. Crack closure was monitored for the small surface cracks and found to decrease with crack growth in these tests.

Introduction

The study of the growth behaviour of small surface fatigue cracks has taken a major role in the fatigue literature within the past decade. The so-called 'small crack effect', in which crack growth occurs below the long crack threshold, has been documented in many engineering materials including 7075-T6 aluminium (**1**)(**2**), nickel aluminium bronze (**3**), iron 3% silicon (**4**) and IMI 685 titanium (**5**). However, there has been very little study of the characteristics of small crack growth in steels, especially in the heat treated, or quenched and tempered, condition (**6**)–(**8**). Since steels represent the most widely used structural material, it is essential to examine the similarities and differences between long and small fatigue crack growth in these materials. This paper presents the results of work in progress on small and long cracks in quenched and tempered 4140 steel.

The most common methods used to monitor the growth of small fatigue cracks are optical or scanning electron microscopy of the crack itself or of a surface replica. Unfortunately, only information about the intersection of the crack with the surface is obtained. The surface acoustic wave (SAW) technique employed in the present study allows crack behaviour to be monitored in depth.

* Department of Materials Science and Engineering.
† Department of Mechanical Engineering, Stanford University, Stanford, CA 94305

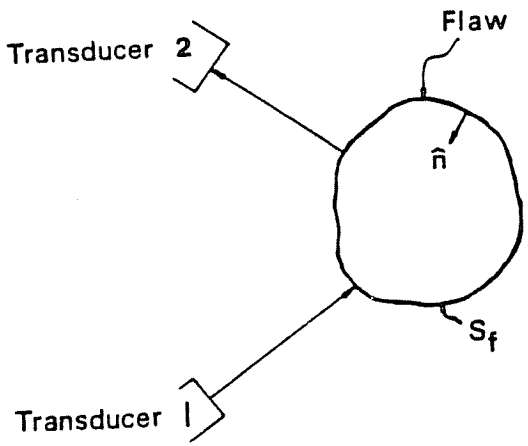

Fig 1 Schematic of generalized scattering of acoustic waves from a flaw. Transducer 1 emits the waves which are received at transducer 2 (14)

The technique is based on the acoustic scattering theory of Kino (**9**) and Auld (**10**) which treats the reflection of acoustic waves from a flaw within a material (Fig. 1). The ratio of the amplitude of the scattered signal received at transducer 2 to that input to the sending transducer 1 is known as the reflection coefficient S_{21}, and

$$S_{21} \equiv \frac{A_2}{A_1} = \frac{j\omega}{4P} \int_{S_f} u_j \sigma_{ij} \hat{n}_i \, dS \tag{1}$$

For an explanation of the terms in the acoustic equations see Appendix 1.

Equation (1) is greatly simplified when considering a surface acoustic wave travelling in the z direction normal to a semi-elliptical surface crack in the xy plane whose depth, a, is much smaller than the acoustic wavelength. In this case the crack resides in a SAW stress field with the component of stress σ_{zz}. The other components of stress can be neglected relative to σ_{zz}. Equation (1) then reduces to

$$S_{21} = \frac{j\omega}{4P} \int_{S_c} \Delta u_z \sigma_{zz} \, dS \tag{2}$$

So, the reflection coefficient for a surface crack can be measured from information regarding the stress field of the surface acoustic wave along with a few experimental parameters.

In order to apply the acoustic theory to an actual surface fatigue crack more development is necessary. Resch *et al.* (**11**)–(**14**) have shown that the crack depth and crack closure stress can be measured using the acoustic technique. The crack depth can be determined from a measurement of the surface length,

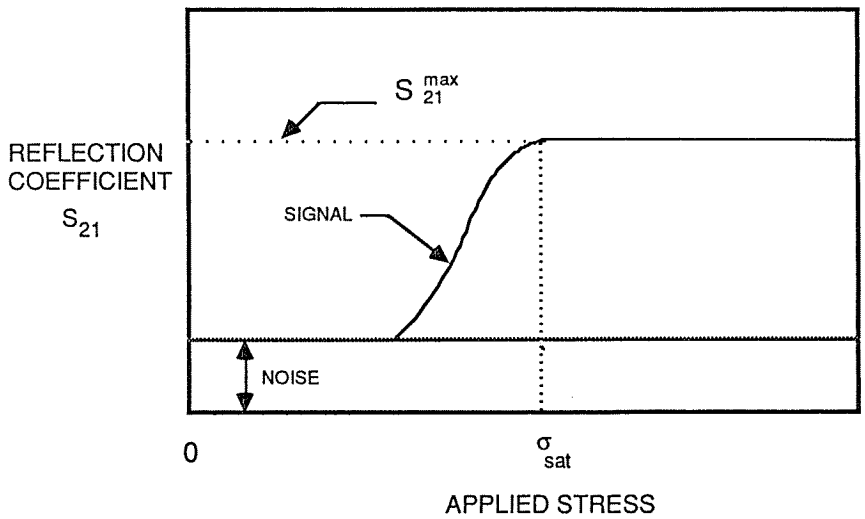

Fig 2 Acoustic measurement of crack closure stress. The stress at which the acoustic signal saturates (σ_{sat}) corresponds to the closure stress

$2c$, and the reflection coefficient, S_{21}. The crack closure stress can be measured as described below. The accuracy of crack depth prediction has been shown to be within 20 per cent of the actual crack depth for cracks 50–200 μm in depth in a range of materials (**14**). Details concerning implementation of the acoustic technique can be found in reference (**14**).

The above discussion shows that, theoretically, there is a direct relationship between the reflection coefficient and the crack depth. An empirical correlation between the reflection voltage, a quantity proportional to the reflection coefficient and measured directly on the laboratory oscilloscope, and crack depth has also been developed for the material, microstructure, and sample geometry of this study. This aids prediction of crack depth in the laboratory.

The measurement of crack closure stress may be an even more valuable aspect of the technique than measurement of depth. Figure 2 shows the behaviour of the acoustic signal as a tensile stress is applied to a specimen containing a surface crack. If a closure stress is present, the crack will be tightly closed in the absence of an applied stress. The reflection from such a closed crack is below the 'noise' level of the measurement system. This 'noise' is caused by electronic amplification of the signal and scattering of the surface waves by the microstructure (e.g., grain boundaries) of the material. As stress is applied, the crack begins to open. This appears as an increase in the acoustic reflection signal. The signal continues to increase with stress until it saturates. This saturation stress (σ_{sat}) corresponds to the stress at which the crack is completely open in depth, i.e., the crack closure stress. This is illustrated in

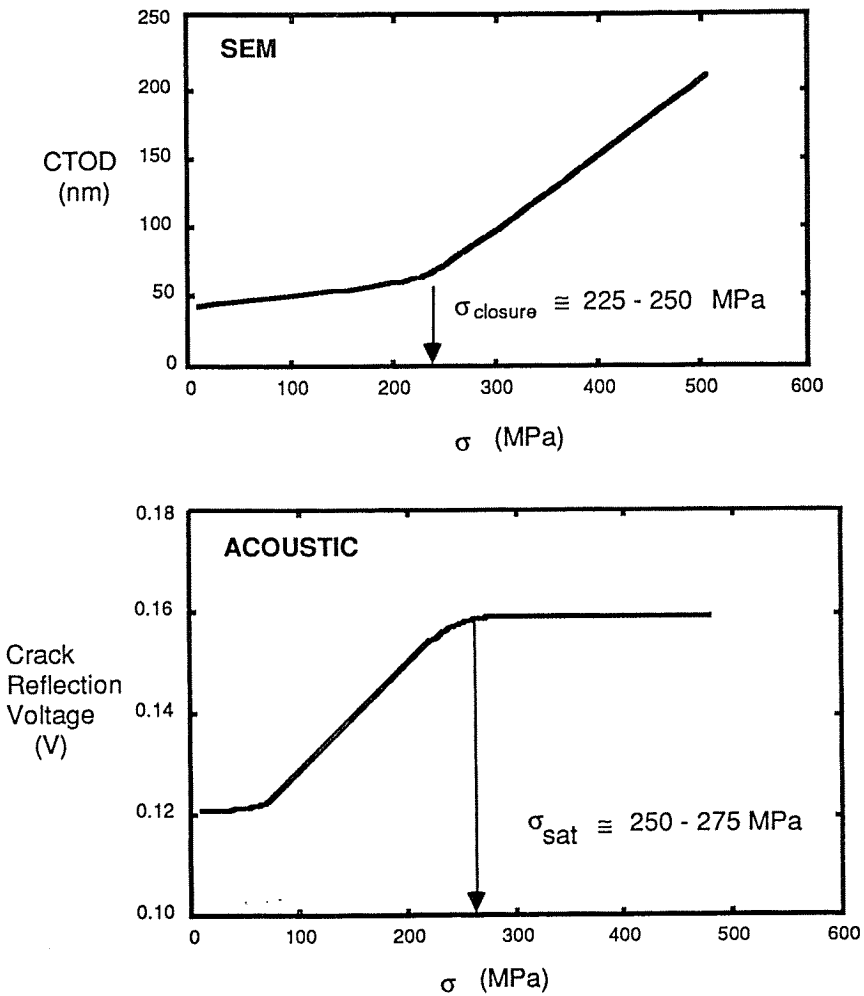

Fig 3 Comparison of the acoustic measurement of the crack closure stress with that determined by crack tip compliance measured in a scanning electron microscope (SEM)

Fig. 3 where the dependency of CTOD measured in the SEM and of acoustic response to the applied stress are compared. The stress at which the crack tip compliance changes corresponds to the crack closure stress (**15**). This value correlates well with σ_{sat}.

To summarize the use of surface acoustic waves to monitor small crack behaviour some advantages and disadvantages can be cited. Crack depth and closure stress can be accurately measured and monitored continuously during

crack growth. The technique is extremely sensitive with a measurement resolution of 3 μm crack growth. It is viable for many materials including quenched and tempered high strength steel, age hardened aluminium, and ceramics. There are some disadvantages to the technique. Only one isolated fatigue crack can be monitored in a given sample. An array of cracks would cause multiple reflections which the present theory cannot treat. Also, only a limited range of crack sizes from 70 to 200 μm can be studied at present. The reflections from smaller cracks are below the 'noise' of the measurement system and larger cracks are beyond the limits of the theory for the SAW frequency used. Working within these limitations, however, the acoustic technique is a valuable method for the study of small surface cracks.

Experimental procedures

A schematic diagram of the major components of the surface acoustic wave system is shown in Fig. 4. A function generator produces a sine wave at 3 MHz which is then gated to 3 wavelengths duation. The signal is amplified and serves as the input to the sending transducer. Each transducer consists of a small slice of piezoelectric PZT crystal held at a specific angle by an RTV silicone wedge. The wedge is cast into a hard polymer block and the entire ensemble measures only 13 × 12 × 11 mm. A low viscosity diagnostic medical ultrasonic fluid is used as a coupling medium. The incoming signal causes the PZT crystal to produce a longitudinal wave which travels through the RTV silicone. The angle of the crystal is such that when the longitudinal wave encounters the specimen surface it is converted to a surface, or Rayleigh, wave. The wave packet then travels away from the transducer in a narrow beam approximately 4 mm wide. The beam reflects from the microcrack, if the crack is sufficiently open as described above, and travels back to the receiving transducer. This signal is then amplified and monitored on an oscilloscope.

The material used in this study was AISI 4140 steel of chemical composition (per cent weight) C 0.38, Mn 0.86, P 0.004, S 0.004, Si 0.23, Cr 0.90, and Mo 0.18. It was chosen because of the ease with which it could be heat treated to various microstructures and due to its wide industrial use. This particular grade of 4140 has very low phosphorous and sulfur contents producing a very clean microstructure.

All heat treatments of the fatigue specimens were performed in vacuum to prevent surface decarburization which could affect small crack growth. Samples were austenitized at 850°C for 1 hour and oil quenched. The specimens were then tempered for 1 hour at either 200, 400, 550, or 700°C to produce a range of yield strengths and microstructures. The microstructures varied from very lightly tempered martensite (200°C temper, R_c = 54, σ_y = 1600 MPa) to a heavily tempered, slightly spheroidized structure (700°C temper, R_c = 26, σ_y = 875 MPa). The intermediate Rockwell hardness levels were 45 and 38 R_c.

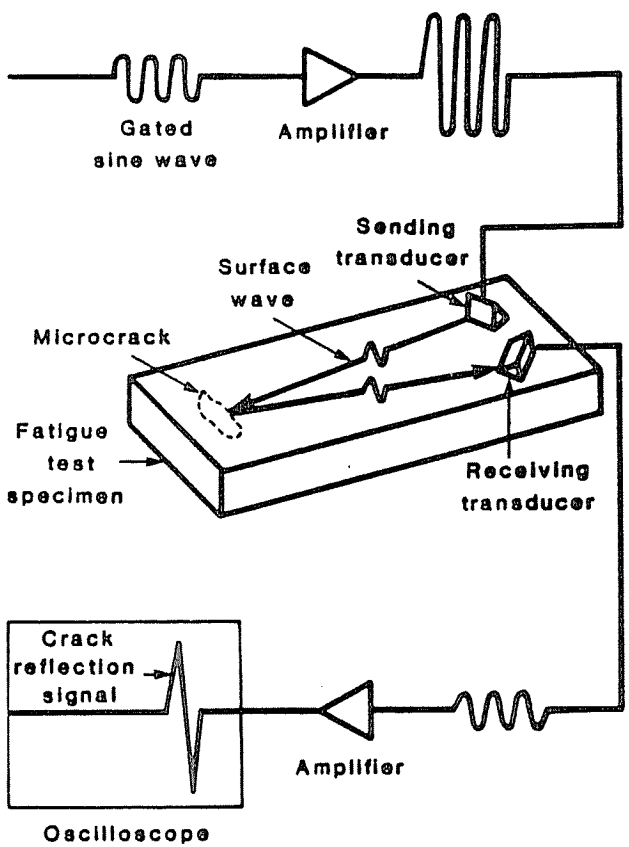

Fig 4 Schematic of the surface acoustic wave system used to monitor the growth of small surface fatigue cracks (16)

Each structure possessed the same prior austenite grain size of approximately 10–15 μm.

In order to utilize the acoustic technique to study small cracks in the heat treated 4140 steel, a special sample design and crack initiation technique had to be developed (**16**). Several major characteristics of the cantilevered bending fatigue sample (Fig. 5) are as follows. The design is compatible with the acoustic technique, meaning no unwanted reflections from specimen boundaries are produced that could interfere with the crack reflection signal. The tapered cross-section produces a small region of high stress on the specimen surface and minimizes corner cracking that could occur in a rectangular cross-section. The overall sample size is small enough to fit into a typical SEM chamber to allow high resolution studies of the cracks. A single, isolated fatigue

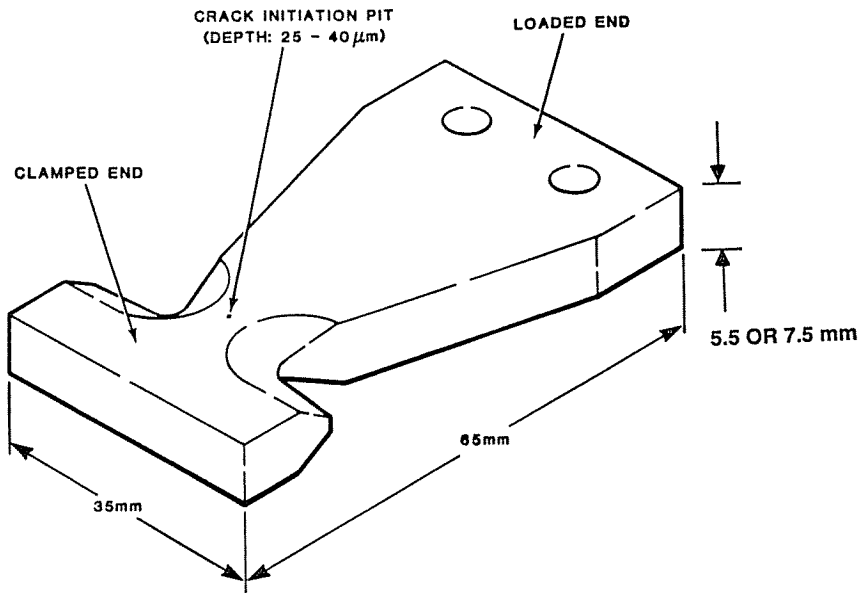

Fig 5 Cantilevered bending fatigue specimen used for the small crack studies

crack is initiated from a small surface pit 25–40 μm in depth. The pit is produced by an electro-spark cutting machine using an extremely sharp electrode. Samples were tempered following pitting to minimize any residual stresses introduced by the spark machining. The transducers are placed at the large end of the sample pointing toward the pit and initiated crack. A simple 'C-clamp' device holds the transducers on the specimen for the entire testing period, allowing crack behaviour to be monitored continuously. A strain gauge on the back face of the sample measures the strain from which the stress was calculated. The compliance of the specimens was not affected by the small cracks on the top surface.

All small and long crack tests were performed on a servo-hydraulic testing machine. The small crack samples were cycled under $R = 0$ conditions at 3–8 Hz, depending on the loading required, in stroke control. Cracks could only be initiated when a maximum cyclic stress was 70–85 per cent of the yield strength of the material. Cracks allowed to grow at this stress level would do so at well above threshold rates. Since the interesting region of small crack growth occurs near-threshold, the load was shed in 20 or 10 per cent increments, depending on the stress level, until near-threshold growth rates were achieved. The cracks were then allowed to grow under constant maximum stress conditions. Data on small crack growth was taken following the load shedding procedure. During load shedding, care was exercised to insure that the crack had grown beyond

the plastic zone of the previous loading step. The crack depth and closure stress (σ_{sat}) were measured acoustically. The value of ΔK for the small cracks was calculated using $\Delta K = 1.32\Delta\sigma\sqrt{a}$ as in reference (**2**).

Long crack tests were done with compact tension samples (63.5 × 61 × 6.35 mm) under $R = 0.05$ conditions. Near-threshold growth data and the threshold values (ΔK_{th}) were obtained using K-decreasing test procedures (**17**). Crack length was measured optically using a travelling microscope.

Results

Figure 6 shows the da/dN–ΔK behaviour for long through-cracks in compact tension samples at near threshold growth rates for the four tempering temperatures. The threshold values are given in Table 1. Increasing the tempering temperature is associated with an increase in ΔK_{th}. This effect has also been documented in 300M steel by Ritchie (**18**).

Table 1 Effect of tempering on long crack thresholds

Tempering temperature (°C)	ΔK_{th} ($MPa\sqrt{m}$)
200	2.80
400	3.50
550	7.20
700	8.50

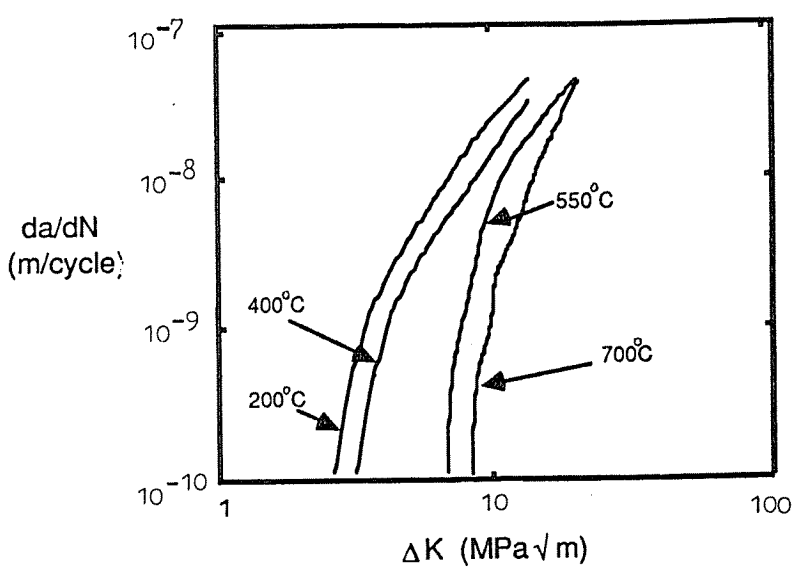

Fig 6 Long crack growth near the threshold region for the four tempering temperatures indicated

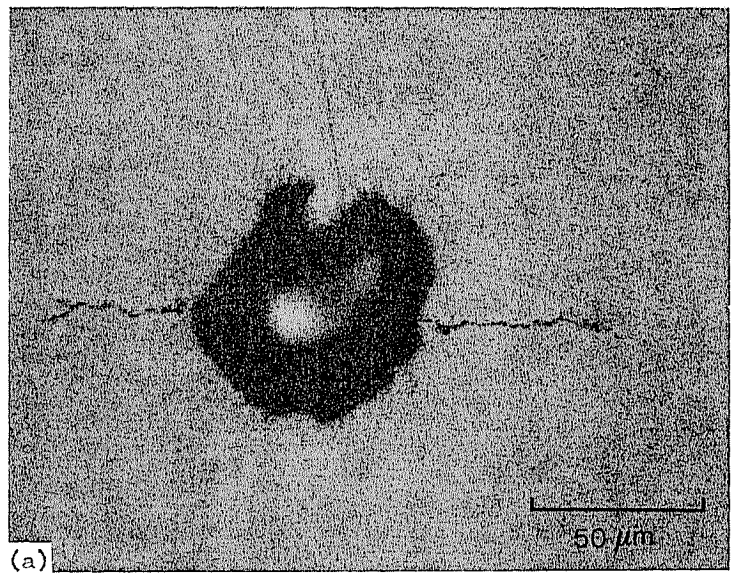

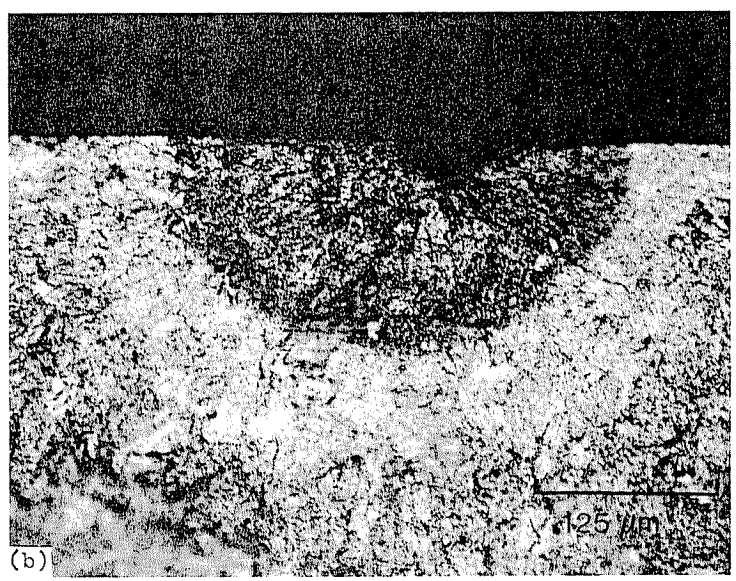

Fig 7 The appearance of small surface cracks (a) initiated from the starter pit on the surface and (b) as an oxidized profile showing a nearly semi-circular crack front

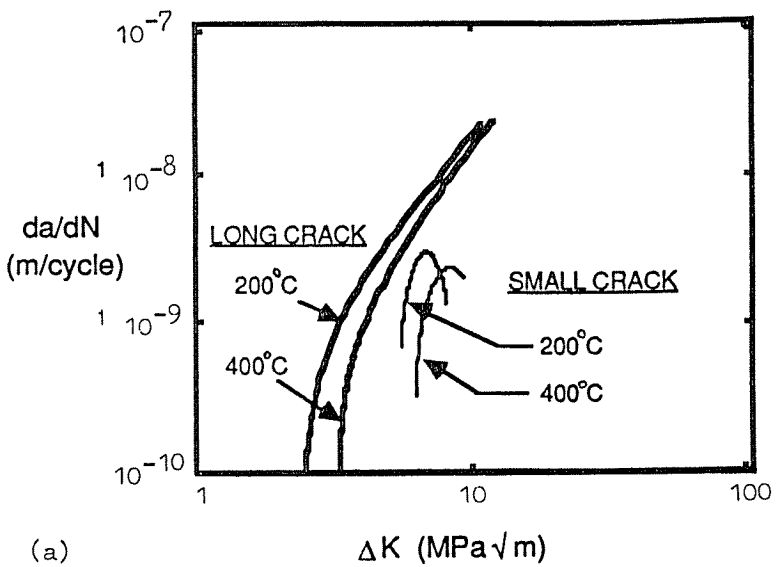

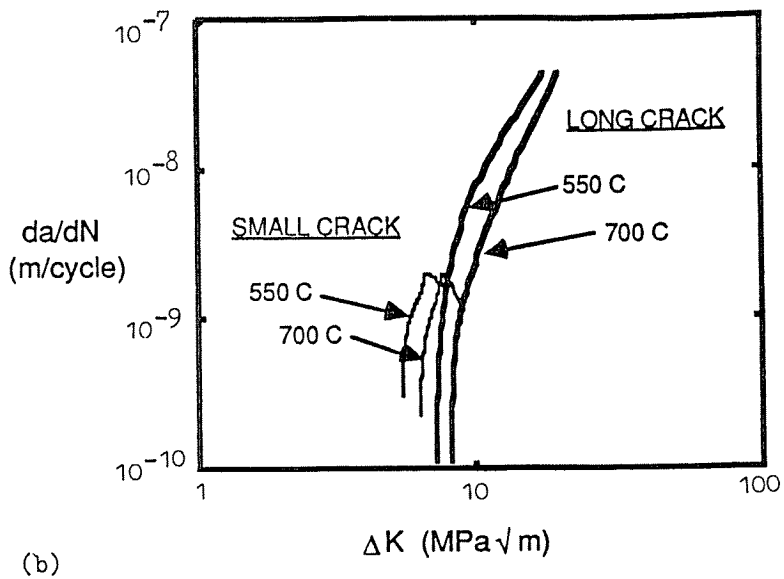

Fig 8 Comparison of long crack growth with small crack growth (a) for the lower tempering temperatures, and (b) for the higher tempering temperatures

Before presenting the small crack growth results, it is worthwhile to examine the appearance of these cracks on the surface and in depth (Fig. 7). On the surface the cracks are shown to grow from both sides of the small pit. By oxidizing a cracked sample at 300°C for 20 minutes in air and then fatiguing the sample in two, the profile of the crack is marked by a thin oxide layer. The cracks grow in a semi-circular fashion. This crack profile, also seen in other materials (1), persists up to a depth of 250 μm in this particular sample design. Once the crack is initiated, the pit does not seem to affect crack growth.

The small crack growth results are best presented in comparison to the long crack data. At the lower tempering temperatures of 200 and 400°C (Fig. 8(a)) the small cracks grow at ΔK levels significantly above the long crack threshold. For these samples, the small cracks are actually growing slower than their long crack counterparts. The higher tempering temperatures, 550 and 700°C, show the opposite behaviour (Fig. 8(b)). Small cracks grow at ΔK levels below their respective long crack threshold values; small crack growth for these tempering treatments shows the so-called 'small crack effect'. The small and long crack curves did not superpose for any of the tempering treatments at near-threshold growth rates. An interesting finding is that all the small crack da/dN–ΔK curves show a growth rate maximum. This is presently under investigation; it occurs for all the tempering treatments.

The crack closure results for the small surface cracks show another interesting trend. Figure 9 shows the crack closure history for a single crack in a sample

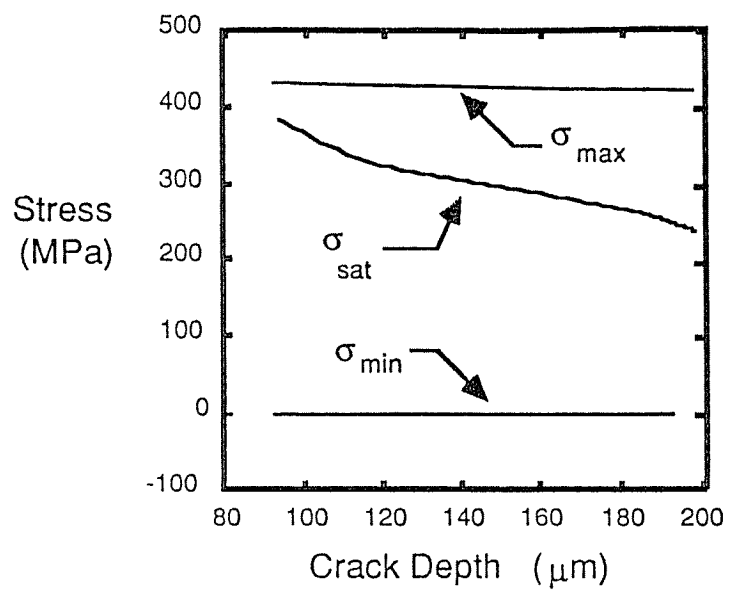

Fig 9 Crack closure results for a single growing small surface crack. σ_{max} is the maximum cyclic stress, $\sigma_{min} = 0$ and σ_{sat} is the acoustically measured crack closure stress

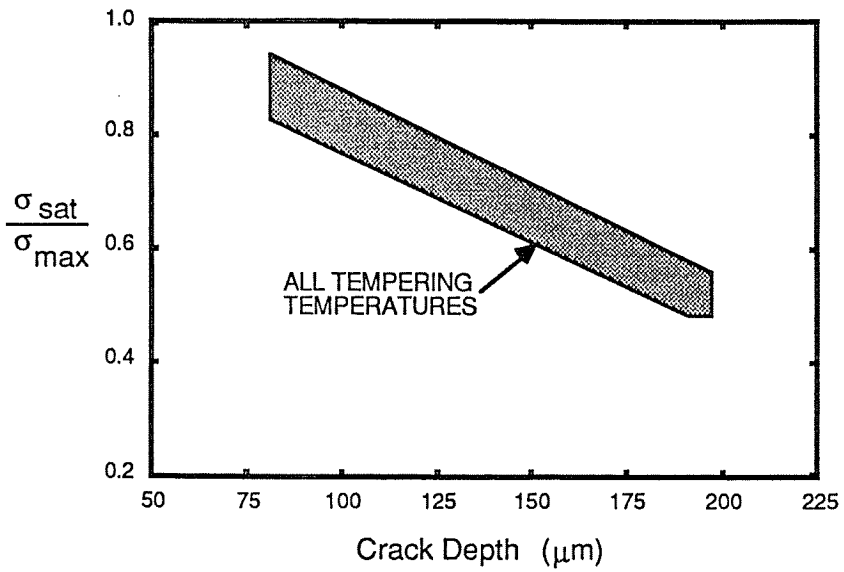

Fig 10 Normalized closure stress versus crack depth for all tempering temperatures studied

tempered at 550°C. The bending stress gradient is taken into account in the σ_{max} and σ_{sat} curves. The closure stress decreases with crack growth for the crack size regime (75–200 μm depth) studied. Similar behaviour was documented for all tempering treatments (Fig. 10). The closure stress begins as a very high percentage of σ_{max} decreasing to about 50 per cent at a depth of 200 μm. This high level of crack closure causes a low value of the effective stress range and therefore ΔK_{eff}. Experiments are currently underway in order to compare the da/dN–ΔK_{eff} behaviour of long cracks to small cracks.

Discussion

The two major aspects of the surface acoustic wave technique are the prediction of crack depth and measurement of crack closure stress. Since the small cracks in these tests grew as half circles, one could have used optical methods to determine the crack depth. However, many times cracks are very difficult to see optically whereas they are readily detected acoustically. Thus, even when the depth of the small cracks is simply half the surface length, acoustic detection still has advantages over optical methods. The rapid and accurate determination of crack closure is perhaps the major contribution of the acoustic technique to fatigue research. In a matter of minutes the acoustic method can measure what it takes other methods (e.g., compliance measurement in the SEM) hours to do.

The results for long crack growth are not unexpected, however, there is not a simple explanation for the increase in ΔK_{th} with increasing tempering temperature (decreasing yield strength). The increase in the ductility of the structures tempered at higher temperatures may be a major factor. This could cause the mode of failure to change drastically from, for example, cleavage to ductile rupture. Work is currently underway to document the fracture morphology for each tempering treatment. Variation in the amount of crack closure could also contribute to the different thresholds measured. Experiments to measure the level of crack closure for the long cracks are in progress. The curves for all four tempering treatments begin to merge at higher growth rates. This follows the well-documented trend of a decreased influence of microstructure on long crack growth well above the threshold (**19**).

The small crack growth results show several interesting features. The trend observed above in the long cracks is preserved, that is, increasing resistance to crack growth with increasing tempering temperature. However, the difference between 200°C and 700°C tempers is much less than would be expected based on the long crack studies. This may indicate that diffent factors control the growth of long cracks compared to small cracks in this material. Further study is underway to investigate this.

There are two results from the small crack investigations which are particularly puzzling; the maximum in the da/dN–ΔK curves and the decreasing level of crack closure. The reasons for the growth rate maximum observed in small crack growth are not presently known. It is not caused by an increase in the crack closure stress since this decreases as the crack grows. A changing crack profile is not responsible since post fracture studies indicate a semi-circular crack front up to the maximum depth studied. It may be merely a transient which develops when the small crack curve begins to merge with the long crack curve. This seems to occur for the 500° and 700°C tempers. The continuously decreasing level of crack closure with crack growth was a consistent finding for all the tempering temperatures studied. Many small crack studies in the literature have documented the opposite effect – increasing closure stress with crack growth (**4**)(**6**)(**20**)–(**22**). The fact that the crack sizes studied here were somewhat larger that the studies referenced above may be involved with the explanation for the decreasing closure stress. It is not yet clear why closure should decrease as crack growth occurs. Detailed studies are presently underway to determine the mechanical or microstructural variables responsible for these effects.

The importance of rapid small crack growth below the long crack threshold has been well-documented in the literature (**1**)–(**8**). Using long crack growth behaviour in design may yield non-conservative crack growth estimates. In quenched and tempered 4140 steel this effect occurs as the yield strength is decreased (samples tempered at higher tempering temperatures). The magnitude of this small crack effect is not as large as reported in other alloys (**1**)(**2**)(**5**). It is, however, important to realize that this effect can be produced in the same

alloy system by varying the microstructure and, in this case, the yield strength. The underlying reasons may be based on the variation in microstructure from very lightly tempered martensite to a nearly spheroidized structure. Identification and characterization of the relevant microstructural features controlling crack growth are currently underway. It is hoped that these studies will shed more light on the reasons for the small crack effect in this alloy system.

Conclusions

(1) A surface acoustic wave ultrasonic technique was shown to be capable of measuring both the crack depth and closure stress for small surface cracks in quenched and tempered 4140 steel.

(2) ΔK_{th} for long through-cracks in compact tension samples increased from 2.8 to 8.5 MPa$\sqrt{m}$ as the tempering temperature increased from 200 to 700°C. The increase in tempering temperature caused a decrease in yield strength from 1600 to 875 MPa.

(3) Small surface crack growth in specially designed cantilevered bending fatigue samples showed slower growth rates at the same ΔK as the tempering temperature was increased (decreasing yield strength). The differences in small crack growth with tempering temperature were not as great as would be expected based on the long crack studies.

(4) Comparison between long cracks and small cracks showed the following trends. The small crack and long crack growth curves did not superpose for any of the tempering treatments.
   (a) At the lower tempering temperatures (200, 400°C), small cracks grew at ΔK levels above their corresponding long crack thresholds.
   (b) At the higher tempering temperatures (550, 700°C), small cracks grew at ΔK levels below their corresponding long crack thresholds.

(5) The level of crack closure for small surface cracks decreased from 85–90 per cent of the maximum applied stress to 50–60 per cent when crack growth occurred from 75 to 200 μm in depth under constant maximum cyclic stress conditions.

Acknowledgements

The support of the following people and organizations is greatly appreciated: Dr A. D. Wilson of the Lukens Steel Company, Coatesville, Pennsylvania for donating the high quality 4140 steel used for this investigation, the IBM corporation, San Jose, California for the use of a high resolution SEM with which to monitor the crack tip compliance, the Office of Naval Research for providing a fellowship to Mr London, and the US Department of Energy for a research contract, with Dr Stanley Wolf as technical monitor, under which this study was done.

Appendix: Explanation of terms in acoustic equations

S_{21}	reflection coefficient
A_2, A_1	amplitude of acoustic waves scattered from the flaw and input to the sending transducer measured at the transducer terminals
j	$\sqrt{-1}$
ω	angular frequency of the acoustic wave (rad/sec)
P	power input to the sending transducer
S_f	flaw surface
u	acoustic displacement field at the flaw surface
σ	acoustic stress field
$\hat{n}$	inward directed normal to the flaw surface
S_c	crack surface

References

(1) LANKFORD, J. (1982) The growth of small fatigue cracks in 7075-T6 aluminum, *Fatigue Engng mater. Structures*, **5**, 233–248.
(2) LANKFORD, J. (1983) The effect of environment on the growth of small fatigue cracks, *Fatigue Engng mater. Structures*, **6**, 15–31.
(3) TAYLOR, D. and KNOTT, J. F. (1981) Fatigue crack propagation behaviour of short cracks; the effect of microstructure, *Fatigue Engng Mater. Structures*, **4**, 147–155.
(4) TANAKA, K., HOJO, M., and NAKAI, Y. (1983) Fatigue crack initiation and early propagation in 3% silicon iron, *ASTM STP 811*, p. 207.
(5) BROWN, C. W. and HICKS, M. A. (1983) A study of short fatigue crack growth behavior in titanium alloy IMI 685, *Fatigue Engng Mater. Structures*, **6**, 67–76.
(6) BREAT, J. L., MUDRY, F., and PINEAU, A. (1983) Short crack propagation and closure effects in A508 steel, *Fatigue Engng Mater. Structures*, **6**, 349–358.
(7) DOWLING, N. E. (1983) Growth of short fatigue cracks in an alloy steel, American Society of Mechanical Engineers 4th National Congress on Pressure Vessel and Piping Technology, Portland, Oregon.
(8) JAMES, M. N. and SMITH, G. C. (1983) Crack closure and surface microcrack thresholds – some experimental observations, *Int. J. Fractures*, **5**, 75.
(9) KINO, G. S. (1978) The application of reciprocity theory to scattering of acoustic waves by flaws, *J. Appl. Phys.*, **49**, 3190.
(10) AULD, B. A. (1979) General electromechanical reciprocity relations applied to the calculation of elastic wave scattering coefficients, *Wave Motion*, **1**, 3.
(11) RESCH, M. T., SHYNE, J. C., KINO, G. S., and NELSON, D. V. (1982) Long wavelength Rayleigh wave scattering from microscopic surface fatigue cracks, *Review of Progress in Quantitative Nondestructive Evaluation* (Edited by Thompson, D. O. and Chimenti, D. E.) (Plenum Press, New York), vol. 1, p. 573.
(12) RESCH, M. T., NELSON, D. V., SHYNE, J. C. and KINO, G. S. (1983) Acoustic monitoring of small surface fatigue crack growth, *Advances in Crack Length Measurement* (Edited by Beevers, C. J.) (EMAS, West Midlands).
(13) RESCH, M. T. (1982) *Nondestructive evaluation of small surface cracks using surface acoustic waves*, Doctoral dissertation, Stanford University, Stanford, CA.
(14) RESCH, M. T., LONDON, B., RAMUSAT, G. F., YUCE, H. H., NELSON, D. V., and SHYNE, J. C. (1985) A surface acoustic wave technique for monitoring the growth behavior of small surface fatigue cracks, *J. Nondestructive Eval.* (in press).
(15) MORRIS, W. L. (1977) The early stages of fatigue crack propagation in aluminum 2048. *Metall. Trans A*, **8A**, 589.
(16) LONDON, B. (1985) New specimen design for studying the growth of small fatigue cracks with surface acoustic waves, *Rev. Sci. Instrum.*, **56**, 1632.

(17) American Society for Testing and Materials (1978) Tentative test method for constant-load-amplitude fatigue crack growth rates above 10^{-8} m/cycle, ASTM Specification E647–78T. Also: Proposed ASTM test method for measurement of fatigue crack growth rates (specification under development).
(18) RITCHIE, R. O. (1977) Influence of microstructure on near-threshold fatigue-crack propagation in ultra-high strength steel, *Metal Science*, Aug./Sept., 368.
(19) IMHOF, E. J. and BARSOM, J. M. (1973) Fatigue and corrosion-fatigue crack growth of 4340 steel at various yield strengths, *ASTM STP 536*, p. 182.
(20) MORRIS, W. L. (1977) Crack closure load development for surface microcracks in aluminum 2219-T851, *Metall. Trans A*, **8A**, 1079.
(21) TANAKA, K. and NAKAI, Y. (1983) Propagation and non-propagation of short fatigue cracks at a sharp notch, *Fatigue Engng Mater. Structures*, **6**, 315.
(22) RITCHIE, R. O. and SURESH, S. (1982) Mechanics and physics of the growth of small cracks, Proceedings of the 55th Meeting of the AGARD Structural and Materials Panel on Behavior of Short Cracks in Airframe Components, Toronto, Canada.